

Size-independent growth of pure zinc blende GaAs nanowires*

Ye Xian(叶显)[†], Huang Hui(黄辉), Guo Jingwei(郭经纬), Ren Xiaomin(任晓敏),
Huang Yongqing(黄永清), and Wang Qi(王琦)

(Key Laboratory of Information Photonics & Optical Communication, Ministry of Education,
Beijing University of Posts and Telecommunications, Beijing 100876, China)

Abstract: Pure zinc blende GaAs nanowires were grown by metal organic chemical vapor deposition on GaAs (111) B substrates via Au catalyzed vapor-liquid-solid mechanism. We found that the grown nanowires are rod-like in shape and have a pure zinc blende structure; moreover, the growth rate is independent on its diameters. It can be concluded that, direct impingement of vapor species onto the Au–Ga droplets contributes to the growth of the nanowire; in contrast, the adatom diffusion makes little contribution. The results indicate that the droplet acts as a catalyst rather than an adatom collector, larger diameter and high supersaturation in the droplet leads to the pure zinc blende structure of the nanowire.

Key words: GaAs nanowire; supersaturation; pure zinc blende structure; metalorganic chemical vapor deposition

DOI: 10.1088/1674-4926/31/7/073001

PACC: 7280E

1. Introduction

Semiconductor nanowires (NWs) have drawn much attention due to their potential applications for nanoscale electronics, photonics and sensing^[1,2]. GaAs NWs can be grown via selective area epitaxy growth (SAEG), self-catalyzed, or Au assisted vapor-liquid-solid (VLS) mechanism^[3–10]. For the VLS mechanism, the NWs growth was related with the direct impingement of the precursors onto the Au–Ga droplets surface, supersaturation of the species in the droplet, the adatom diffusion from the surface of substrate and sidewalls to the droplet^[8, 11, 12]. NW growth models by the VLS mechanism can be grouped into two categories, the classic VLS models and diffusion-induced models. NWs formed by the diffusion-induced model usually show a tapering shape at their roots, and the NW length decreases with its radius^[5, 7, 8]. In the opposite case of the classic VLS growth, where semiconductor particles can impinge only on the drop surface, the NW length increases with the radius^[8, 10, 11]. In most cases, the growth rate of NWs is a function of its diameter. However, there are few reports of diameter independent growth of NWs^[13]. Moreover, the grown NWs normally have defects such as twins or stacking faults, and NWs with small radii (< 50 nm) tend to exhibit wurtzite (WZ) crystal structure^[9, 12, 14–18]. In most cases, the WZ phase of III–V NWs is not stable and exhibits highly faulted WZ–ZB mix-ups^[12, 14]. For utilizing predictable and reproducible NW devices in future applications, optimal control of the morphology, crystal structure, absolute control of growth rates and understanding the growth properties are required. Further investigations of NW growth mechanism are of paramount importance to determine the morphology and growth rate of NWs^[12, 14].

In this paper, the dependence of the diameter and diffusion of vapor precursors on NWs growth were investigated. The related growth mechanism was discussed.

2. Experiment

The epitaxial growth of GaAs NWs was performed by metal organic chemical vapor deposition (MOCVD) with a Thomas Swan CCS-MOCVD system at a pressure of 100 Torr. Trimethylgallium (TMGa) and arsine (AsH₃) were used as precursors. The carrier gas was hydrogen. The sample was prepared by first depositing an Au film with a thickness of 4 nm on the GaAs (111) B substrate by magnetron sputtering. Then the Au-coated GaAs substrate was loaded into the MOCVD reactor and annealed in situ at 650 °C under arsine ambient for 300 s to form the Au–Ga alloyed particles as catalyst. Finally, NWs growth was carried out at 440 °C for 600 s with V/III ratio of 70.

Atom force microscopy (AFM) was used to analyze the size distribution and density of the Au–Ga particles after the annealing process. Morphologies of the NWs were characterized by field-emission scanning electron microscopy (FE-SEM, JEOL JSM-5500). The crystal structure of the NWs was investigated by transmission electron microscopy (TEM, FEI Tecanai F30). TEM specimens were prepared by ultrasonically dispersing NWs in ethanol for 5 min and then dispersing the NWs onto holey carbon grids.

3. Results and discussion

Figure 1(a) shows the atomic force microscopy (AFM) images of the Au–Ga particles on the GaAs substrate after annealing. Figure 1(b) shows the histogram of size distributions

* Project supported by the Basic Research on Compatible Heterogeneous Integration and Functional-Microstructure Assemblage for the Development of Novel Optoelectronic Devices, China (No. 2010CB327600), the 111 Program of China (No. B07005), the Program of Key International Science and Technology Cooperation Projects (No. 2006DFB11110), the New Century Excellent Talents in University (NCET-08-0736), the National High Technology R & D Program of China (Nos. 2009AA03Z405, 2009AA03Z417), the Chinese Universities Scientific Fund (Nos. BUPT2009RC0409, BUPT2009RC0410), and the Program for Changjiang Scholars and Innovative Research Team in University, MOE (No. IRT0609).

[†] Corresponding author. Email: shineyea@foxmail.com

Received 6 June 2009, revised manuscript received 25 February 2010

© 2010 Chinese Institute of Electronics

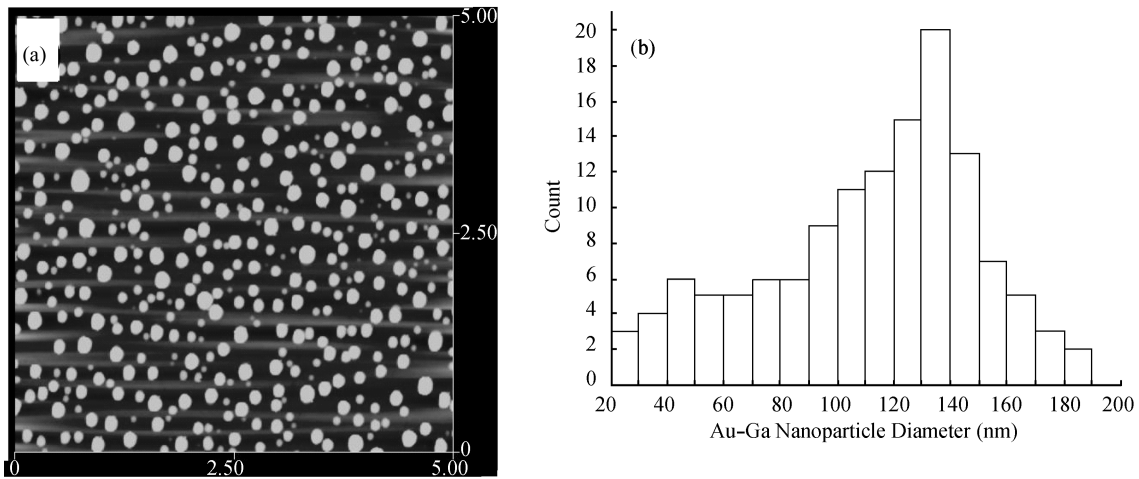


Fig. 1. AFM images of Au–Ga particles annealed from gold film and histogram of its diameter distributions on the GaAs (111) B surface.

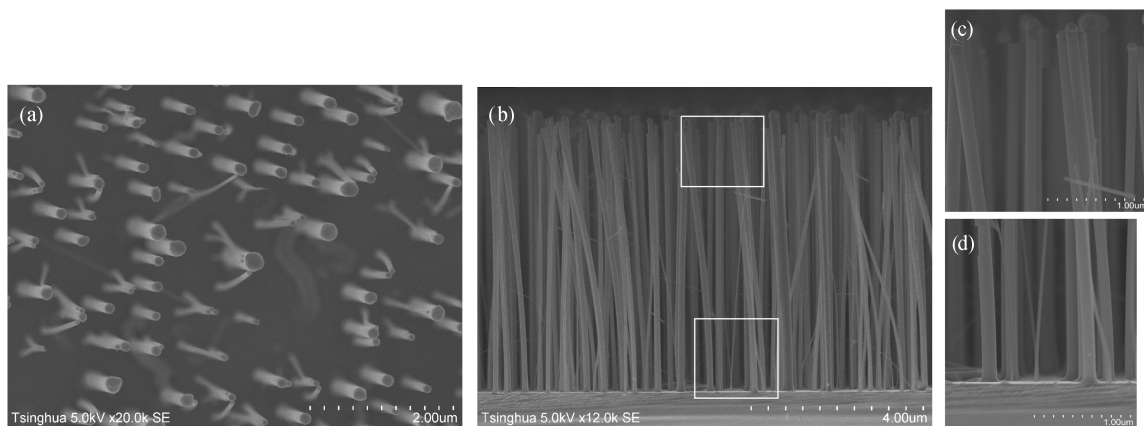


Fig. 2. SEM images of GaAs NWs.

of Au–Ga particles. As seen from Figs. 1(a) and 1(b), there is a rather broad size distribution of Au–Ga particles diameters in the sample, the diameters of the particles range from 20 to 200 nm with the corresponding density of Au–Ga droplets is $2.2 \times 10^9 \text{ cm}^{-2}$. Dispersal of the size distribution is due to random agglomeration of Au atom.

Planar and cross sectional FE-SEM images of the grown GaAs NWs are shown in Figs. 2(a) and 2(b), respectively. The average NW length for the sample is about $6.3 \mu\text{m}$. It can be found that the lengths of NWs are almost the same, despite the broad distribution of the diameters (determined by the corresponding size of the droplet as shown in Fig. 1. In other words, the growth rate of NWs is independent on their diameters. Moreover, the tip and base images of the NW with same higher magnification were seen in Figs. 2(c) and 2(d), respectively. It can be seen that the NW diameters are uniform from base to top and approximately the same as the diameters of Au–Ga droplets.

For VLS growth, there are two major contributions, i.e., direct impingement of the precursors onto the alloy droplet and adatom diffusion from the sidewalls and substrate surface to the top^[8–11]. For the diffusion-induced growth modes, NWs show a tapering or pencil-like shape due to lateral overgrowth, when its length is longer than the diffusion length of adatoms, and

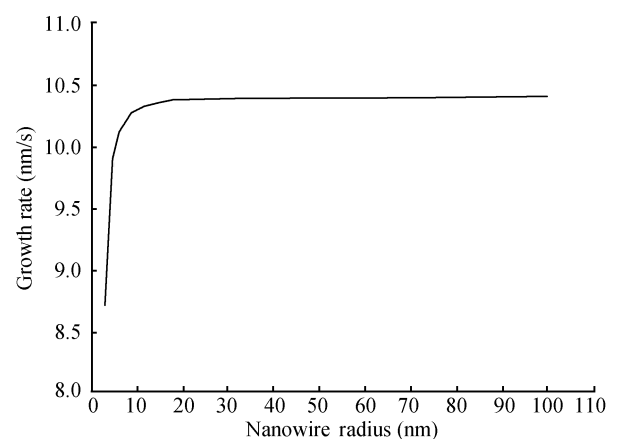


Fig. 3. Nanowire radius versus growth rate.

the growth rate was dependent on the diameter^[7–9,11,19–21].

In our case, the length of NWs is about $6 \mu\text{m}$, which is much larger than the Ga surface diffusion length (typical diffusion length is less than $2 \mu\text{m}$ for MOCVD at 450°C)^[21]. Thus, it can be concluded that catalytic pyrolysis of the precursors impinging onto the Au–Ga droplets is the main contribution to the growth of the long and uniform NWs, while the adatom dif-

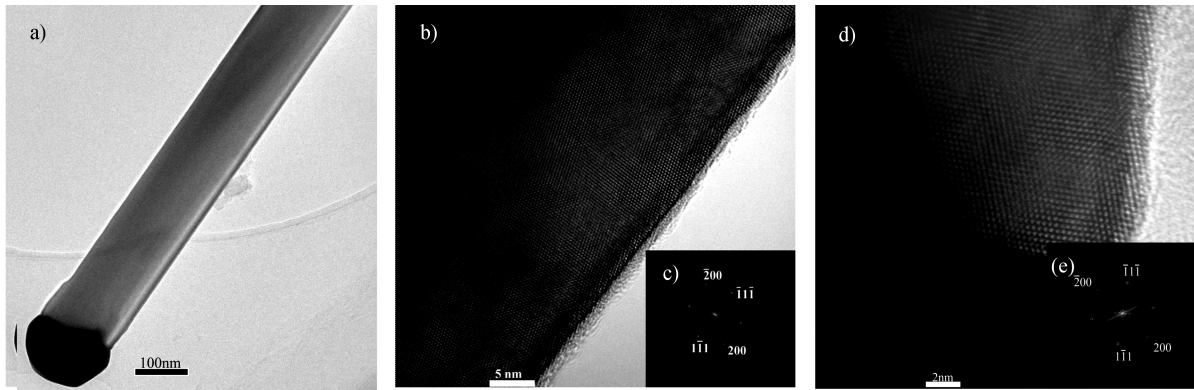


Fig. 4. TEM images of NW with diameter of 139 nm.

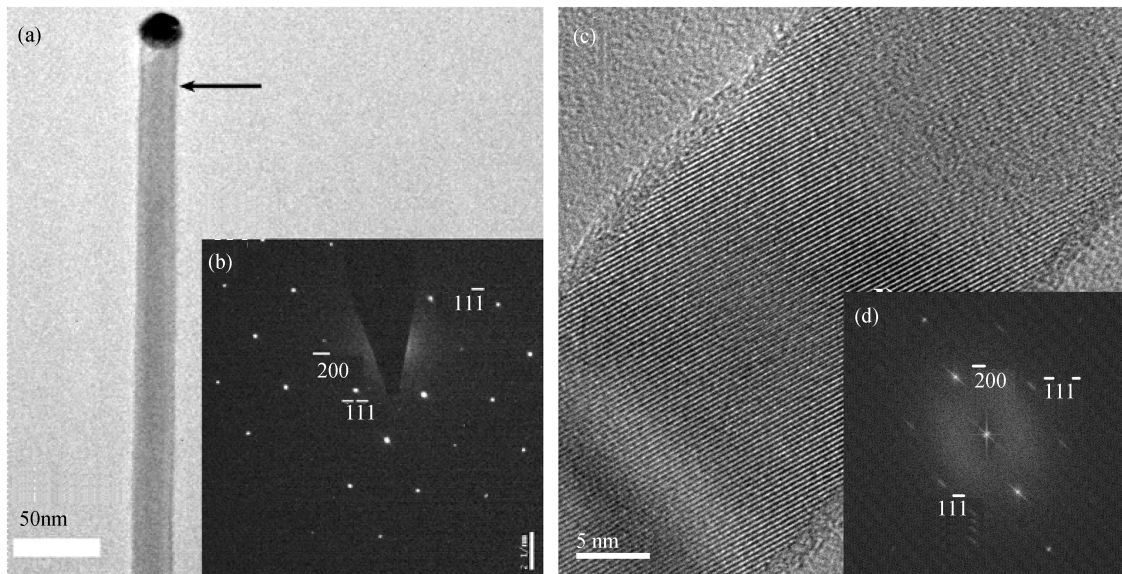


Fig. 5. TEM images of NW with diameter of 24 nm.

fusion does little contributions in our case. In other words, the droplets act as a catalyst rather than an adatom collector.

As shown in Fig. 2, the growth rate was 10.5 nm/s. These values are quite high compared to the Au-assisted MBE of GaAs NWs, where the growth rate is typically of order of 1 nm/s^[10]. A high growth rate of ~ 10 nm/s relates to high liquid supersaturation, due to the irreversible decomposition of the metalorganics precursor on the droplet surface, the reactant pressure (metal species) outside the particles is persistently high, and the NWs grow in a mode with the time-independent supersaturation most of the time.

In general, the NW growth rate is a function of diameters due to Gibbs-Thomson (GT) effect, or the adatom diffusion from the substrate and sidewalls to the top^[8, 11]. For NWs growth with larger particles and under high supersaturation, the GT effect can be neglected^[8].

For our growth, the number of atoms transferred from the vapor phase to the droplet per unit time is equal to that transformed from liquid to the crystal phase, the growth rate, dL/dt , obeys the following proportionality^[8, 21, 22].

$$\frac{dL}{dt} \propto K[\exp(R/r_c) - \exp(R/r)], \quad (1)$$

where K is kinetics coefficient independent on diameter and growth parameter, and r is the particles radius. The characteristic GT radius R and the critical radius r_c given by^[21, 23]

$$R = 2\sigma\Omega/(k_B T), \quad r_c = 2\sigma\Omega/\Delta\mu, \quad (2)$$

where σ is the surface energy density at the vapor-liquid interface, Ω is the molar volume of the reactant species in the catalyst particles, k_B is the Boltzmann constant, T is growth temperature, and $\Delta\mu$ is the difference of chemical potentials in the vapor and in the equilibrium liquid phase.

In our case, the growth rate is almost independent of diameter. The higher supersaturations accounts for this peculiar phenomenon. The R in the right hand side of Eq. (1) depends on the temperature and it is a constant at $T = \text{const}$. The reactant pressure of the MOCVD reaction is persistently high due to the mostly irreversible decomposition of the metalorganics^[8].

The supersaturation of the vapor and liquid phases will increase with increasing precursor flows, and high supersaturations will result in smaller r_c . As shown in Fig. 3, for NWs with thinner radius ($r < 10$ nm), the growth rate increases with the radius, while for NWs with larger radius ($r > 10$ nm), the growth rate is almost independent on its diameter due to the

term R/r_c of the Eq. (1) is much larger than the term R/r . So, for NWs with larger radius ($r > 10$ nm) grown under this condition, the dependence of diameters can be neglected.

Figure 4(a) shows TEM images of the NW with a diameter of 139 nm. High resolution TEM (HRTEM) images of the NW tip and trunk are shown in Figs. 4(b) and 4(d), respectively. Figures 4(c) and 4(e) show the corresponding fast Fourier transform (FFT) images of NW tip and trunk, respectively. Figure 5 shows TEM images of the NWs with diameter of 24 nm, and the selected area electron diffraction (SAED) pattern of the region near the Au catalyst was shown in Fig. 5(b). Figure 5(c) illustrates HRTEM images of its trunk, and the corresponding FFT image of the wire was shown in Fig. 5(d). All NWs were of a zinc blend structure and the growth direction is $\langle 111 \rangle$ and zone axis is $\langle 110 \rangle$. It is quite surprising that pure zinc blend crystal structure without any stacking faults or rotational twins is seen in the NWs with diameters of 139 and 24 nm, because usually GaAs thinner than 50 nm in radius are predominantly WZ with highly faulted WZ/ZB mix-up sections^[9, 12, 14–18].

Fluctuations in supersaturation of the droplet would lead to stacking faults or twins in the wire^[5, 24–26]. The fluctuation can be induced by the Ga adatom diffusion from the sidewall and substrate surface, because the amount of adatom diffusing into the droplet varies with lateral overgrowth as well as wire length^[24–26]. In our case, the absence of adatoms diffusion contribution in growth process would result in more stable supersaturation in the droplet, so high crystal quality NWs can be obtained.

4. Conclusions

In summary, we have synthesized GaAs NWs by MOCVD on GaAs (111) B substrates via Au catalyzed vapor–liquid–solid mechanism. The diameters distribution of Au–Ga particles, growth mechanism, crystal structure, and growth rate of the NWs was studied. The grown NWs are rod-like in shape and the growth rate is independent of its diameters. Pure zinc blende GaAs nanowires without defects were obtained. The NW was grown with main contributions from direct impingement of vapor species onto the Au–Ga droplets and the adatom diffusion makes little contribution. Our results provide insight into the physical processes controlling the growth of NWs via VLS mechanism, it indicates that the droplet acts as a catalyst rather than an adatom collector, larger diameter and high supersaturation in the droplets lead to size-independent growth of NWs. The results should enable the development of the nanowires with uniform shape and pure crystal structure, and axial nanowires heterostructures. It will therefore be beneficial not only for GaAs nanowires but also for other III–V nanowires.

References

- [1] Huang Y, Duan X, Cui Y, et al. Logic gates and computation from assembled nanowire building blocks. *Science*, 2001, 294: 1313
- [2] Bryllert T, Wernersson L E, Lowgren T, et al. Vertical wrap-gated nanowire transistors. *Nanotechnology*, 2006, 17: S227
- [3] Ikejiri K, Sato T, Yoshida H, et al. Growth characteristics of GaAs nanowires obtained by selective area metal-organic vapour-phase epitaxy. *Nanotechnology*, 2008, 19: 265604
- [4] Jabeen F, Grillo V, Rubini S, et al. Self-catalyzed growth of GaAs nanowires on cleaved Si by molecular beam epitaxy. *Nanotechnology*, 2008, 19: 275711
- [5] Joyce H J, Gao Q, Tan H H, et al. High purity GaAs nanowires free of planar defects: growth and characterization. *Adv Funct Mater*, 2008, 18: 3794
- [6] Borgström M, Deppert K, Samuelson L, et al. Size- and shape-controlled GaAs nano-whiskers grown by MOVPE: a growth study. *J Cryst Growth*, 2004, 260: 18
- [7] Soci C, Bao X Y, Aplin D P R, et al. A systematic study on the growth of GaAs nanowires by metal-organic chemical vapor deposition. *Nano Lett*, 2008, 8(12): 4275
- [8] Seifert W, Borgström M, Deppert K, et al. Growth of one-dimensional nanostructures in MOVPE. *J Cryst Growth*, 2004, 272: 211
- [9] Plante M C, LaPierre R R. Au-assisted growth of GaAs nanowires by gas source molecular beam epitaxy: tapering, sidewall faceting and crystal structure. *J Cryst Growth*, 2008, 310: 356
- [10] Harmand J C, Tchernycheva M, Patriarche G, et al. GaAs nanowires formed by Au-assisted molecular beam epitaxy: effect of growth temperature. *J Cryst Growth*, 2007, 301/302: 853
- [11] Dubrovskii V G, Sibirev N V, Cirilin G E, et al. Gibbs-Thomson and diffusion-induced contributions to the growth rate of Si, InP, and GaAs nanowires. *Phys Rev B*, 2009, 79: 205316
- [12] Johansson J, Karlsson L S, Dick K A, et al. Effects of supersaturation on the crystal structure of gold seeded III–V nanowires. *Cryst Growth and Design*, 2009, 9: 766
- [13] Kodambaka S, Tersoff J, Reuter M C, et al. Diameter-independent kinetics in the vapor–liquid–solid growth of Si nanowires. *Phys Rev Lett*, 2006, 96: 096105
- [14] Glas F, Harmand J C, Patriarche J. Why does wurtzite form in nanowires of III–V zinc blende semiconductors. *Phys Rev Lett*, 2007, 99: 146101
- [15] Persson A I, Larsson M W, Stengstrom S, et al. Solid-phase diffusion mechanism for GaAs nanowire growth. *Nature Mater*, 2004, 3: 677
- [16] Dick K A, Deppert K, Mårtensson T, et al. Failure of the vapor–liquid–solid mechanism in Au-assisted MOVPE growth of InAs nanowires. *Nano Lett*, 2005, 5: 761
- [17] Patriarche G, Glas F, Tchernycheva M, et al. Wurtzite to zinc blende phase transition in GaAs nanowires induced by epitaxial burying. *Nano Lett*, 2008, 8: 1638
- [18] Shtrikman H, Popovitz-Biro R, Kretinin A, et al. Method for suppression of stacking faults in wurtzite III–V nanowires. *Nano Lett*, 2009, 9: 1506
- [19] Tchernycheva M, Travers L, Patriarche G, et al. Au-assisted molecular beam epitaxy of InAs nanowires: growth and theoretical analysis. *J Appl Phys*, 2007, 102: 094313
- [20] Chen C, Plante M C, Fradin C, et al. Layer-by-layer and step-flow growth mechanisms in GaAsP/GaP nanowire heterostructures. *J Mater Res*, 2006, 21: 2801
- [21] Kim Y, Joyce H J, Gao Q, et al. Influence of nanowire density on the shape and optical properties of ternary InGaAs nanowires. *Nano Lett*, 2006, 6: 599
- [22] Johansson J, Wacaser B A, Dick K A, et al. Growth related aspects of epitaxial nanowires. *Nanotechnology*, 2006, 17: 355
- [23] Chen Z, Cao C. Effect of size in nanowires grown by the vapor–liquid–solid mechanism. *Appl Phys Lett*, 2006, 88: 143118
- [24] Joyce H J, Gao Q, Tan H H, et al. Unexpected benefits of rapid growth rate for III V nanowires. *Nano Lett*, 2009, 9: 695
- [25] Johansson J, Karlsson L S, Patrik C, et al. Structural properties of 111 B oriented III V nanowires. *Nature Mater*, 2006, 5: 574
- [26] Hao Y, Meng G, Wang Z, et al. Periodically twinned nanowires and polytypic nanobelts of ZnS: the role of mass diffusion in vapor–liquid–solid growth. *Nano Lett*, 2006, 6: 1650